

# Optimizing Locomotion Controllers Using Biologically-Based Actuators and Objectives

## *Supplemental Material*

Jack M. Wang, Samuel R. Hamner, Scott L. Delp, Vladlen Koltun

Stanford University

## 1 Data Collection

We collected marker trajectories, ground reaction forces and moments of 20 subjects (10 male, 10 female; height  $1.72 \pm 0.09$  m; mass  $64.86 \pm 9.62$  kg; age  $28.5 \pm 5$  years) walking and running at multiple speeds on an instrumented treadmill. Data was collected while each subject walked at 1.00, 1.25, 1.50, and 1.75 m/s and ran at 2.0, 3.0, 4.0, and 5.0 m/s. Subjects had 54 reflected markers placed on anatomical landmarks during a static calibration trial [5], then functional joint movements were captured to calculate hip joint centers [2]. Static markers were then removed and trajectories of 38 markers were measured during the trials. Marker positions were measured at 100 Hz using eight Vicon MX40+ motion capture cameras. The ground reaction forces and moments were measured at 1000 Hz using a Bertec Corporation fully instrumented treadmill. Marker positions and ground reaction forces were low pass filtered at 15 Hz with a 4th order critically damped filter [6]. A 12 segment, 29 degree-of-freedom musculoskeletal model [4] was used to calculate joint angles and joint moments for each subject. The model's segment lengths were scaled to match the anthropometry based on experimentally measured markers placed on palpable anatomical landmarks and calculated hip joint centers. A virtual marker set was placed on each model based on these same anatomical landmarks. For each trial, inverse kinematics (IK) calculated joint angles and inverse dynamics calculated joint moments (i.e., torques) given joint angles and measured ground reaction forces. Scaling, IK, and inverse dynamics were performed using the OpenSim software package [7].

## 2 MTU Contraction Dynamics

The following relations hold true for our MTU model:

$$F^{\text{CE}} = aF^0 f_l(\tilde{l}^{\text{CE}}) f_v(\tilde{v}^{\text{CE}}), \quad (1)$$

$$F^{\text{MTU}} = F^{\text{CE}} + F^{\text{PE}}, \quad (2)$$

$$l^{\text{MTU}} = l^{\text{CE}} + l^{\text{SE}}, \quad (3)$$

$$F^{\text{MTU}} = F^{\text{SE}} = F^{\text{CE}} + F^{\text{PE}}, \quad (4)$$

$$F^{\text{PE}} = F^{\text{HPE}} - F^{\text{LPE}}. \quad (5)$$

More specifically,

$$F^{\text{HPE}} = F^0 \left\{ 0.56^{-1} (\tilde{l}^{\text{CE}} - 1) \right\}_+^2, \quad (6)$$

$$F^{\text{LPE}} = F^0 \left\{ 0.28^{-1} (0.44 - \tilde{l}^{\text{CE}}) \right\}_+^2, \quad (7)$$

$$F^{\text{SE}} = F^0 \left\{ 0.04^{-1} (\tilde{l}^{\text{SE}} - 1) \right\}_+^2, \quad (8)$$

$$f_l(\tilde{l}^{\text{CE}}) = \exp \left[ \ln(0.05) \left( 0.56^{-1} (\tilde{l}^{\text{CE}} - 1) \right)^4 \right], \quad (9)$$

$$f_v(\tilde{v}^{\text{CE}}) = \begin{cases} \frac{-10 - \tilde{v}^{\text{CE}}}{-10 + 5\tilde{v}^{\text{CE}}}, & \text{if } \tilde{v}^{\text{CE}} < 0 \\ 1.5 + 0.5 \frac{-10 + \tilde{v}^{\text{CE}}}{37.8\tilde{v}^{\text{CE}} + 10}, & \text{if } \tilde{v}^{\text{CE}} \geq 0 \end{cases}, \quad (10)$$

	SOL	TA	GAS	VAS	HAM	RF	GLU	HFL
$F^0$	4000	800	1500	6000	3000	1000	1500	2000
$l^{\text{opt}}$	3.7	5.6	4.7	7.5	9.4	7.5	10.3	10.3
$l^{\text{slk}}$	24.3	22.5	37.4	21.5	29.0	28.1	12.2	9.4
mass	0.63	0.19	0.30	1.90	1.20	0.32	0.65	0.87
$\lambda$	0.81	0.70	0.54	0.50	0.44	0.423	0.50	0.50
$r_1$	4.7	3.7	4.7	5.6	7.5	9.4	9.4	9.4
$r_2$	-	-	4.7	-	4.7	5.6	-	-
$\varphi_1^M$	$\pi/2 - 1.92$	$\pi/2 - 1.40$	$\pi - 2.44$	$\pi - 2.88$	-	-	-	-
$\varphi_1^R$	$\pi/2 - 1.40$	$\pi/2 - 1.92$	$\pi - 2.88$	$\pi - 2.18$	$\pi - 2.71$	0	$\pi - 2.62$	0
$\varphi_2^M$	-	-	$\pi/2 - 1.92$	-	0	$\pi - 2.88$	-	-
$\varphi_2^R$	-	-	$\pi/2 - 1.40$	-	0	$\pi - 2.18$	-	-
$\rho$	0.5	0.7	0.7	0.7	0.7	0.7	0.5	0.5

Table 1: MTU physiological and geometric parameters.  $F^0$  is the maximum isometric force (N),  $l^{\text{opt}}$  is the optimal fiber length (cm), and  $l^{\text{slk}}$  is the tendon slack length (cm). The muscle masses (kg) are estimated by multiplying  $l^{\text{opt}}$  by muscle cross sectional area and assuming a density of  $1060 \text{ kg/m}^3$ , and  $\lambda$  is the fraction of Type I fibers in a given muscle. Parameters  $r_j$ ,  $\varphi_j^M$ ,  $\varphi_j^R$  are joint attachment parameters, and  $\rho$  accounts for pennation angles. Biarticular muscles have two sets of attachment parameters, with  $j = 1$  for the proximal joint. Parameter values are based on Anderson [1], and Geyer and Herr [3], with  $l^{\text{opt}}$ ,  $l^{\text{slk}}$ , and  $r_j$  values scaled to our model’s leg length.

where  $\tilde{l}^{\text{SE}} = l^{\text{SE}}/l^{\text{slk}}$ ,  $l^{\text{slk}}$  is a MTU specific tendon slack length parameter. The remaining variables are defined in Section 3.1 of the main article.  $F^{\text{HPE}}$  and  $F^{\text{SE}}$  model forces generated by stretching the muscle fiber and tendon, respectively.  $F^{\text{LPE}}$  acts to prevent the CE from compressing below reasonable lengths. It follows from (3), (4), (8) that  $F^{\text{MTU}}$  is fully defined by  $l^{\text{MTU}}$  and  $l^{\text{CE}}$ . Note that  $f_v$  assumes a maximum contraction velocity of  $10 l^{\text{opt}}/\text{s}$  for all MTUs.

For a given MTU, the length is defined as

$$l^{\text{MTU}} = l^{\text{opt}} + l^{\text{slk}} + \sum_{j \in \mathcal{J}} \pm \Delta^j(\theta), \quad (11)$$

where  $\mathcal{J}$  is the set of joints attached to the MTU;  $\theta$  is the current joint angle;  $\Delta^j$  captures how the MTU lengths change according to joint angles, its sign depends on whether the MTU extends (+) or flexes (-) the joint. For  $j = \text{hip}$ ,  $\Delta^j(\theta) = \rho r(\theta - \varphi^R)$ , and  $\Delta^j(\theta) = \rho r(\sin(\theta - \varphi^M) - \sin(\varphi^R - \varphi^M))$  for  $j \in \{\text{knee, ankle}\}$ .  $\rho$  accounts for muscle pennation angles,  $\varphi^M$  is defined to be the joint angle with the maximum moment arm, and  $\varphi^R$  is defined to be the joint angle in which  $\Delta^j = 0$ .

Since  $l^{\text{MTU}}$  is completely specified by body configuration,  $l^{\text{CE}}$  is the only remaining quantity needed to compute  $F^{\text{MTU}}$ . We initialize  $l^{\text{CE}}$  to  $l^{\text{opt}}$  at the start of the simulation, and update its value by numerically integrating  $v^{\text{CE}}$ . Equations (2), (4), (5) can be rearranged to give the value of  $f_v$  in terms of the current activation ( $a$ ),  $l^{\text{MTU}}$ , and  $l^{\text{CE}}$ . The analytic form of  $f_v$  can then be readily inverted to give the current  $v^{\text{CE}}$  [3].

### 3 Activation and Maintenance Heat Rates

The muscle activation and maintenance heat rates depend on the mass of the muscle and its fiber composition.

$$\dot{A} = \text{mass} \cdot f_A(u), \quad (12)$$

$$\dot{M} = \text{mass} \cdot g(\tilde{l}^{\text{CE}})f_M(a), \quad (13)$$

where  $\dot{A}$  is activation heat rate,  $\dot{M}$  is maintenance heat rate, mass is muscle mass,  $\tilde{l}^{\text{CE}}$  is normalized muscle fiber length,  $a$  is muscle activation level, and  $u$  is neural excitation level. The metabolic cost of maintaining a given activation level depends on the current muscle fiber length, and is modeled by

$$g(\tilde{l}^{\text{CE}}) = \begin{cases} 0.5, & \text{if } 0 < \tilde{l}^{\text{CE}} \leq 0.5 \\ \tilde{l}^{\text{CE}}, & \text{if } 0.5 < \tilde{l}^{\text{CE}} \leq 1.0 \\ -2\tilde{l}^{\text{CE}} + 3, & \text{if } 1.0 < \tilde{l}^{\text{CE}} \leq 1.5 \\ 0, & \text{if } 1.5 < \tilde{l}^{\text{CE}} \end{cases} \quad (14)$$

Muscle fibers can be categorized into slow and fast types (Types I and II), each with different rates for activation and maintenance. Let  $\lambda$  denote the fraction of Type I fibers in a given muscle, following Anderson [1], we define

$$f_A(u) = 40\lambda \sin\left(\frac{\pi}{2}u\right) + 133(1-\lambda)(1 - \cos\left(\frac{\pi}{2}u\right)), \quad (15)$$

$$f_M(a) = 74\lambda \sin\left(\frac{\pi}{2}a\right) + 111(1-\lambda)(1 - \cos\left(\frac{\pi}{2}a\right)). \quad (16)$$

Equations (15) and (16) account for orderly recruitment of motor units, where slower, Type I fibers are recruited at a faster rate for lower excitation levels.

## 4 Task Terms

The primary task for our locomotion controllers is to move the COM forward for time  $T$  without falling down. A heavy penalty for falling is captured by

$$K_{\text{fail}}(\mathbf{s}_t) = \text{failed}_t, \quad (17)$$

where  $\text{failed}_t = 100$  if the vertical position of the COM falls below 0.7 m at time  $t$ ;  $\text{failed}_t = 0$  otherwise. Note that this definition penalizes falling early more than falling late in the simulation, which is important for the optimization algorithm.

We optimize for the character to move with a target velocity of  $\hat{v}_x - 0.05$  m/s. In particular, we define

$$K_{\text{vel}}(\mathbf{s}_t) = Q(v_x - \hat{v}_x; 0.05) + Q(v_y; 0.05), \quad (18)$$

where  $Q$  is a bounded quadratic penalty defined as  $Q(d, \epsilon) = d^2$  if  $|d| > \epsilon$ , 0 otherwise;  $v_x$  is the character’s forward COM velocity (averaged over the previous step) in the target direction;  $v_y$  is the velocity in the direction perpendicular to the target direction and parallel to the ground plane.

We define tasks for head stabilization by minimizing both the deviation of head orientation from the vertical direction, and the maximum head velocity relative to the COM. Specifically,

$$K_{\text{head}}(\mathbf{s}_t) = 0.1Q(\phi_x^{\text{head}}; 0.05) + 0.1Q(\phi_y^{\text{head}}; 0.05), \quad (19)$$

$$K_{\text{headv}}(\mathbf{s}_t) = 0.1Q(\hat{v}_x^{\text{head}}; 0.15v_x) + 0.1Q(\hat{v}_y^{\text{head}}; 0.2), \quad (20)$$

where  $\phi_x^{\text{head}}$  is the angle between the up vector of the head and the global up vector in the plane defined by the global up vector and the target direction;  $\phi_y^{\text{head}}$  is the angle in the orthogonal plane;  $\hat{v}_x^{\text{head}}$  is the maximum head velocity parallel to the ground plane relative to the COM in the target direction ( $\hat{v}_y^{\text{head}}$  is orthogonal to the target direction) during the previous step.

To maintain an upright posture while pointing the pelvis towards the target direction, we define

$$K_{\text{torso}}(\mathbf{s}_t) = 0.01Q(\phi_z^{\text{pel}} - \phi^{\text{target}}; 0.05) + 0.1Q(\Theta; 0.1), \quad (21)$$

where  $\phi_z^{\text{pel}}$  is the angle between the front vector of the pelvis and the global x-axis projected onto the ground plane;  $\phi^{\text{target}}$  is the angle between the target direction and the global x-axis;  $\Theta$  is the global upper body orientation defined in the main article.

Finally, for both walking and running, each foot should either be in the air or on the ground with more than one point of contact

$$K_{\text{foot}}(\mathbf{s}_t) = \text{unstable}_t^l + \text{unstable}_t^r, \quad (22)$$

where  $\text{unstable}_t^l = 0.001$  if the left foot is on the ground with only one point of contact;  $\text{unstable}_t^r$  is similarly defined for the right foot. Note that all terms are computed at heel-strike and once every 20 timesteps, except  $K_{\text{vel}}$  and  $K_{\text{headv}}$  which are only computed at heel-strike.

## 5 Optimizer Initialization

The starting kinematic state  $(\theta_0, \hat{\theta}_0)$  and joint PD-control parameters  $(k_p, k_d, \theta_d)$  are provided in Table 2. The shaded cells correspond to parameters that are free to be optimized. The parameters listed in the table are for walking control initialization, for running we modify the velocity for `trunk.trans_x` to 3.05 m/s. The initial arm swing parameters (Section 4.4) are specified as follows:  $\theta_e^d = 0.17$  for walking,  $\theta_e^d = 1.915$  for running, and  $\alpha_{\text{arm}} = 0.25$ .

DOF	$\theta_0$	$\hat{\theta}_0$	$k_p$	$k_d$	$\theta_d$	lim <sub>h</sub>	lim <sub>l</sub>
trunk_trans <sub>x</sub>	0	1.3	-	-	-	-	-
trunk_trans <sub>y</sub>	0	0	-	-	-	-	-
trunk_trans <sub>z</sub>	1.32	0	-	-	-	-	-
trunk_orient <sub>x</sub>	0	0	-	-	-	-	-
trunk_orient <sub>y</sub>	5	0	-	-	-	-	-
trunk_orient <sub>z</sub>	0	0	-	-	-	-	-
neck <sub>x</sub>	0	0	100	10	0	60	-60
neck <sub>y</sub>	0	0	100	10	0	50	-80
neck <sub>z</sub>	0	0	100	10	0	80	-80
left_shoulder <sub>x</sub>	0	0	30	3	0	90	-90
left_shoulder <sub>y</sub>	0	0	30	3	-	160	-80
left_shoulder <sub>z</sub>	0	0	30	3	-	20	-20
left_elbow <sub>y</sub>	0	0	30	3	-	120	0
left_elbow <sub>z</sub>	0	0	30	3	0	90	-40
right_shoulder <sub>x</sub>	0	0	30	3	0	90	-90
right_shoulder <sub>y</sub>	0	0	30	3	-	160	-80
right_shoulder <sub>z</sub>	0	0	30	3	-	20	-20
right_elbow <sub>y</sub>	0	0	30	3	-	120	0
right_elbow <sub>z</sub>	0	0	30	3	0	40	-90
back <sub>x</sub>	0	0	300	30	0	5	-5
back <sub>y</sub>	0	0	300	30	0	10	-5
back <sub>z</sub>	0	0	300	30	0	15	-15
left_hip <sub>x</sub>	0	0	1000	100	0	20	-20
left_hip <sub>y</sub>	40	0	-	-	-	165	-
left_hip <sub>z</sub>	0	0	1000	100	-	20	-120
left_knee <sub>y</sub>	5	0	-	-	-	165	-
left_ankle <sub>x</sub>	0	0	30	3	0	35	-2
left_ankle <sub>y</sub>	0	0	-	-	-	-	-
right_hip <sub>x</sub>	0	0	1000	100	0	20	-20
right_hip <sub>y</sub>	5	0	-	-	-	165	-
right_hip <sub>z</sub>	0	0	1000	100	-	120	-20
right_knee <sub>y</sub>	5	0	-	-	-	165	-
right_ankle <sub>x</sub>	0	0	30	3	0	2	-35
right_ankle <sub>y</sub>	5	0	-	-	-	-	-
left_toe <sub>y</sub>	0	0	30	0	0	30	0
right_toe <sub>y</sub>	0	0	30	0	0	30	0

Table 2: Parameters corresponding to model DOFs. The starting kinematic state  $(\theta_0, \hat{\theta}_0)$  and joint PD-control parameters  $(k_p, k_d, \theta_d)$  in shaded table cells are optimized. lim<sub>h</sub> and lim<sub>l</sub> are human-like joint limits enabled in the simulation. Note that the left leg is assumed to be the lead stance leg, and left/right PD-control parameters are swapped on ground contact. Angles are specified in degrees in the table for clarity, but are converted to radians for computation. See Geyer and Herr [3] for how soft joint limits are defined for the sagittal hip, knee, and ankle DOFs.

We set  $\beta = -\frac{13}{48}, \gamma = -\frac{13}{96}$  (not optimized) based on human data. Additionally, the SIMBICON-style coronal hip feedback parameters are initialized to  $c_d = c_v = 0.2$ , and the hip turning parameters ( $\alpha_{\text{hip}}$ ) [9] are initialized to 0.5.

The initial values of the MTU control parameters listed in this section are based on Geyer and Herr [3]. The pre-stimulation values  $p_m, q_m$  are all initialized to 0.01, except  $p_{\text{GLU}} = p_{\text{HFL}} = p_{\text{HAM}} = 0.05$ , and  $p_{\text{VAS}} = 0.08$ .

- Gains of positive force feedback laws:  $G_{\text{SOL}} = 1.2, G_{\text{TA} \leftarrow \text{SOL}} = 0.4, G_{\text{GAS}} = 1.1, G_{\text{VAS}} = 1.2, G_{\text{HAM}} = 0.65, G_{\text{GLU}} = 0.5$ .
- Gains of positive length feedback laws:  $G_{\text{TA}} = 1.1, G_{\text{HFL}} = 0.5, G_{\text{HFL} \leftarrow \text{HAM}} = 4.0$ .
- Offsets of positive length feedback laws:  $H_{\text{TA}} = 0.72, H_{\text{HFL}} = 0.65, H_{\text{HFL} \leftarrow \text{HAM}} = 0.85$ .
- Stance phase PD-control parameters for GLU, HFL, and HAM muscles:  $K_m = 1.91, D_m = 0.2, \theta_m = 0.105$ .
- Swing initiation parameters:  $s_{\text{RF}} = 0.01, s_{\text{VAS}} = 1.0, s_{\text{HFL}} = s_{\text{GLU}} = 0.25$ .
- Stance preparation muscle PD-control parameters:  $K_m = 1.0, D_m = 0.2$ , with common target hip and knee angles initialized to  $\pi - 2.8$  and  $\pi - 3.0$  radians, respectively.
- Stance preparation SIMBICON-style feedback parameters:  $c_d = 0.5, c_v = 0.2$ .
- Swing initialization and stance preparation offsets:  $d_{\text{SI}} = 0.4, d_{\text{SP}} = -0.15$ .
- Additional parameters (defined in Sections 4.2 and 4.3 of the main article) :  $k_{\theta} = 1.15, k_{\theta} = 2.0, \theta_k^{\text{off}} = \pi - 2.97$ .
- Running initialization values are identical to walking, except  $G_{\text{SOL}} = 2.4, G_{\text{GAS}} = 2.2$ .

## 6 Body Model

The zero position and mass distributions of body links and joints are provided in a Matlab data file on the project website<sup>1</sup>. We model the heel and ball of the foot using two cylinders of radius 0.034023, length 0.08. The heel is shifted (-0.0586847, 0, 0.005) from the foot COM, the ball is shifted (0.064702, 0, -0.005) from the foot COM. The toe is modeled as a box with dimensions (0.047432, 0.08, 0.025). The contact parameters in ODE are set based on Wang et al. [8].

## References

- [1] ANDERSON, F. C. *A dynamic optimization solution for a complete cycle of normal gait*. PhD thesis, University of Texas at Austin, 1999.
- [2] GAMAGE, S. S., AND LASENBY, J. New least squares solutions for estimating the average centre of rotation and the axis of rotation. *Journal of Biomechanics* 35, 1 (2002), 87–93.
- [3] GEYER, H., AND HERR, H. A muscle-reflex model that encodes principles of legged mechanics produces human walking dynamics and muscle activities. *IEEE Transactions on Neural Systems and Rehabilitation Engineering* 18, 3 (2010), 263–273.
- [4] HAMNER, S. R., SETH, A., AND DELP, S. L. Muscle contributions to propulsion and support during running. *Journal of Biomechanics* 43 (2010), 2709–2716.
- [5] KADABA, M. P., RAMAKRISHNAN, H. K., AND WOOTTEN, M. E. Measurement of lower extremity kinematics during level walking. *Journal of Orthopaedic Research* 8, 3 (May 1990), 383–392.
- [6] ROBERTSON, D. G. E., AND DOWLING, J. J. Design and responses of Butterworth and critically damped digital filters. *Journal of Electromyography and Kinesiology* 13 (2003), 569–573.
- [7] SETH, A., SHERMAN, M., REINBOLT, J. A., AND DELP, S. L. OpenSim: A musculoskeletal modeling and simulation framework for *in silico* investigations and exchange. In *Proc. Symposium on Human Body Dynamics, Vol. 2* (2011), IUTAM, pp. 212–232.
- [8] WANG, J. M., FLEET, D. J., AND HERTZMANN, A. Optimizing walking controllers. *ACM Transactions on Graphics* 28, 5 (2009).
- [9] WANG, J. M., FLEET, D. J., AND HERTZMANN, A. Optimizing walking controllers for uncertain inputs and environments. *ACM Transactions on Graphics* 29, 4 (2010).

<sup>1</sup><http://graphics.stanford.edu/projects/bio-locomotion>

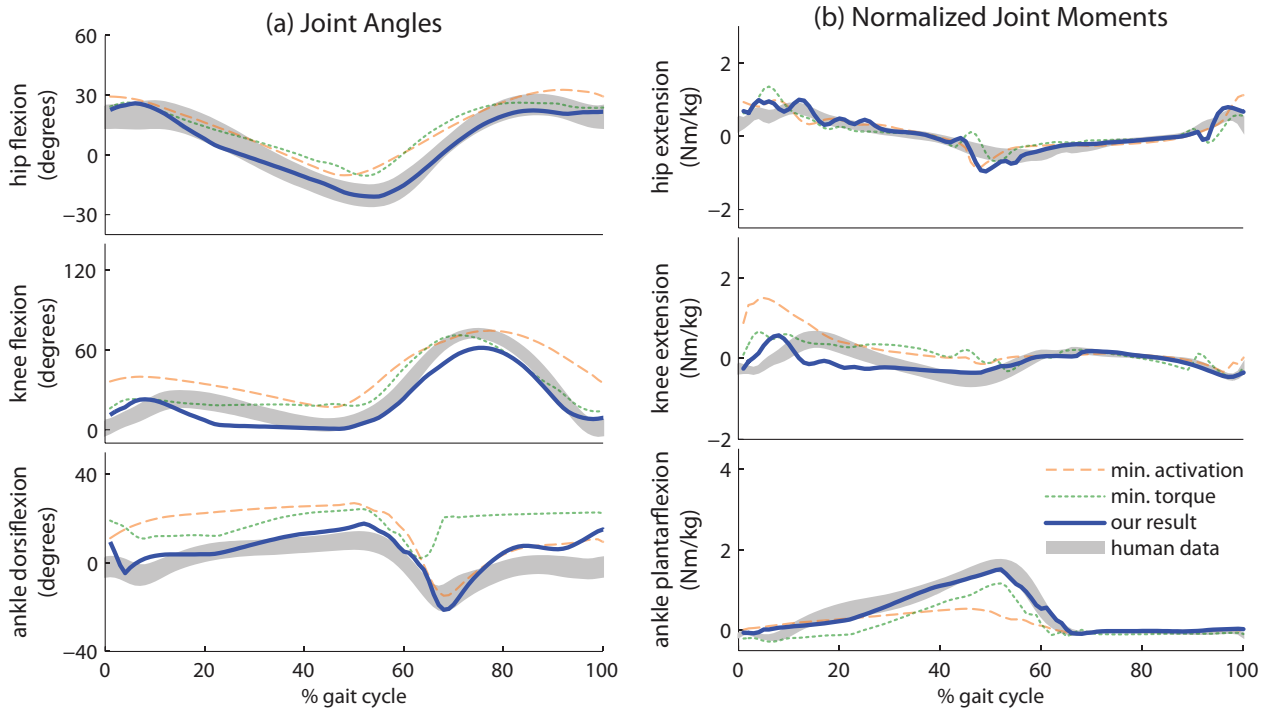


Figure 1: Comparison of simulated gaits to human walking data at 1.25 m/s. The shaded areas represent one standard deviation. *min. activation* is optimized with a squared activations effort term. *min. torque* is optimized with a squared torques effort term. Our result is optimized with the rate of metabolic energy expenditure effort term.

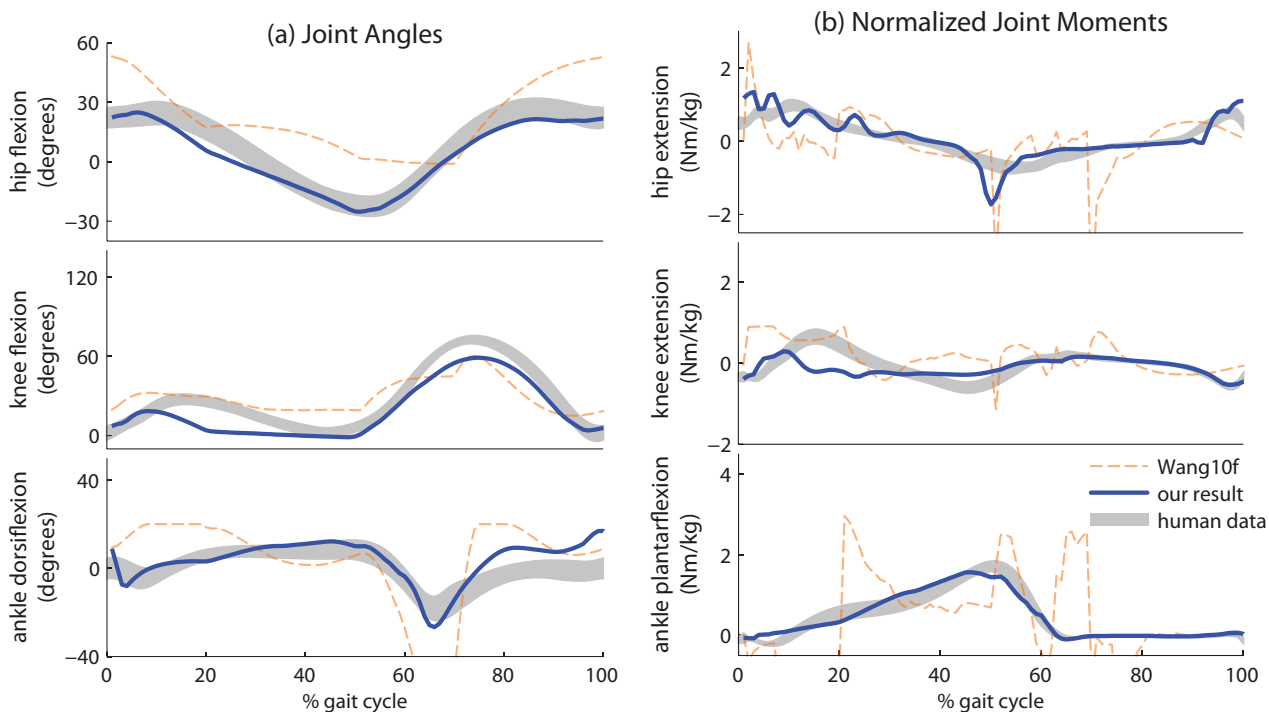


Figure 2: Comparison of simulated gaits to human walking data at 1.5 m/s. The shaded areas represent one standard deviation. *Wang10f* is a controller [9] that moves at 1.6 m/s. Our result is optimized with target velocity 1.5 m/s.

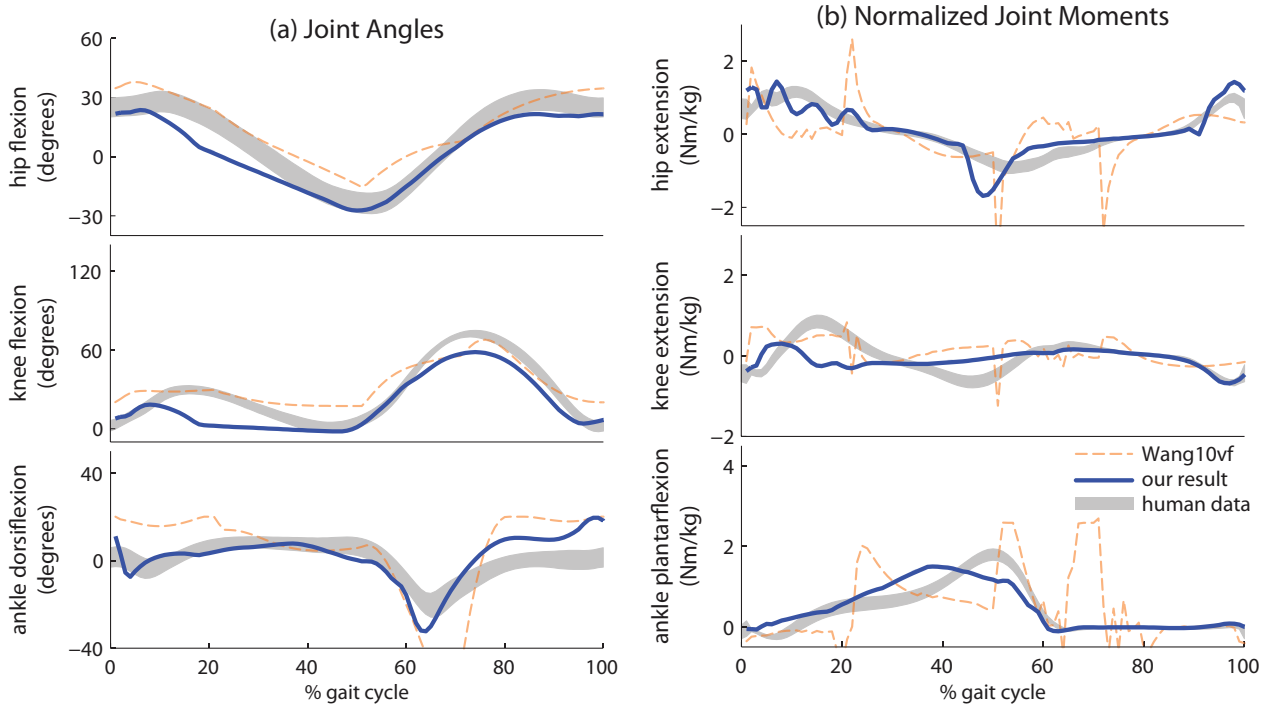


Figure 3: Comparison of simulated gaits to human walking data at 1.75 m/s. The shaded areas represent one standard deviation. *Wang10vf* is an optimized controller [9] that moves at 1.7 m/s. Our result is optimized with target velocity 1.75 m/s.

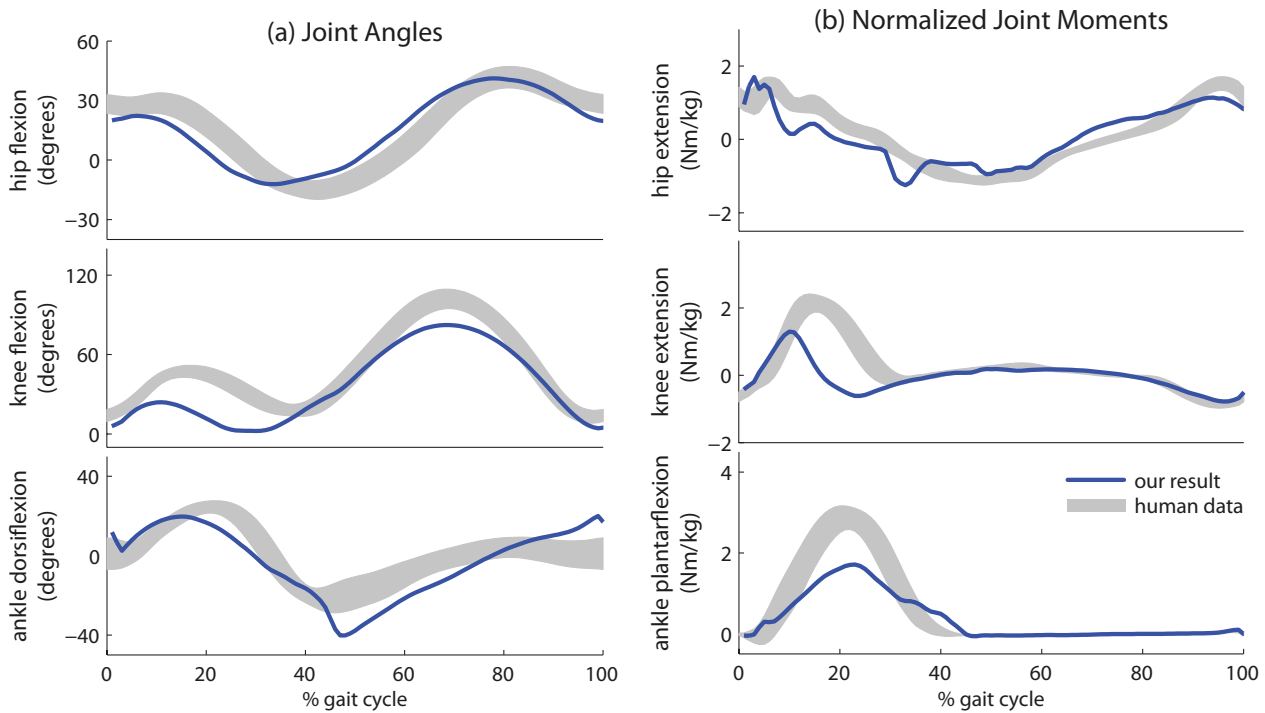


Figure 4: Comparison of simulated gaits to human running data at 3.0 m/s. The shaded areas represent one standard deviation. Our result is optimized with target velocity 3.0 m/s.

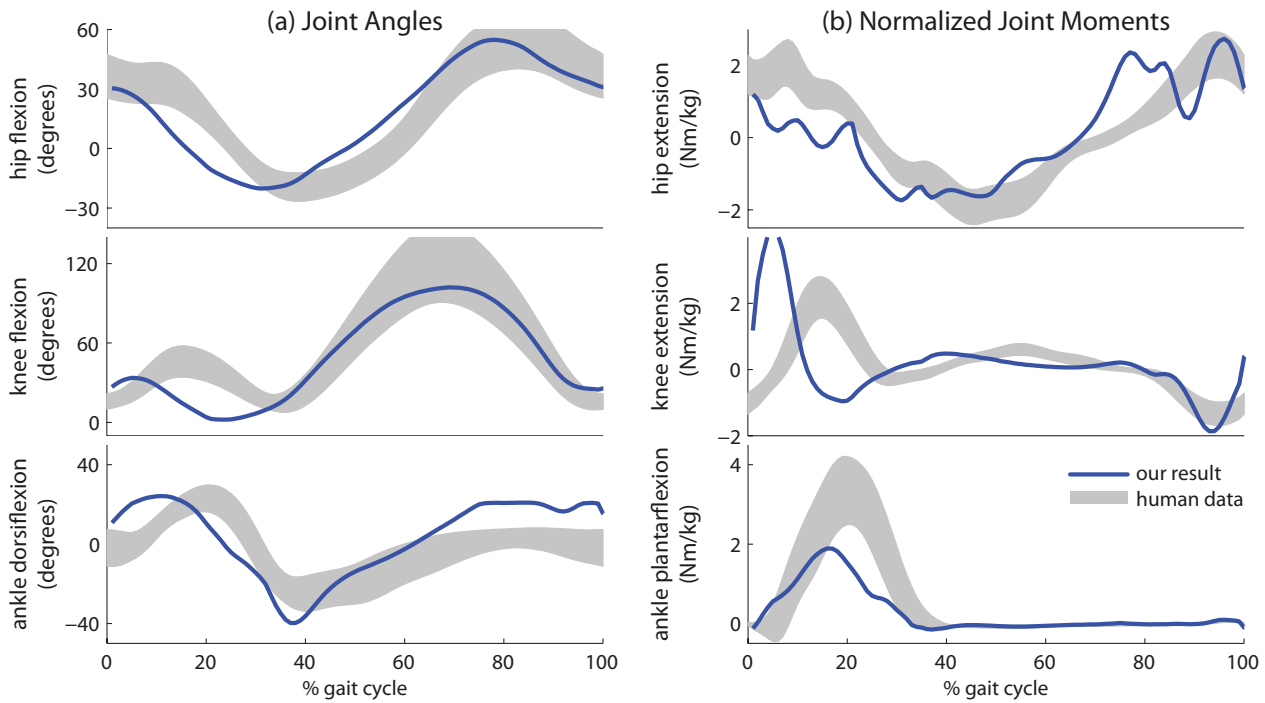


Figure 5: Comparison of simulated gaits to human running data at 5.0 m/s. The shaded areas represent one standard deviation. Our result is optimized with target velocity 5.0 m/s.

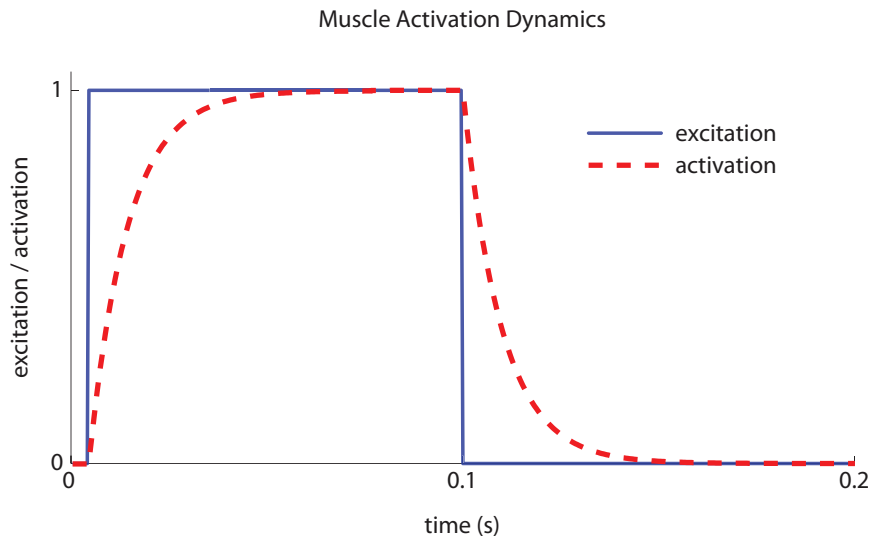


Figure 6: Step-response graph for our activation dynamics. The activation dynamics models conversion of neural excitation ( $u$ ) to muscle activation ( $a$ ), which leads to a first-order delay between the control signal (excitation) and force generation (activation).